NANO LETTERS

2007
Vol. 7, No. 4
981−986

Polarizability of G4-DNA Observed by Electrostatic Force Microscopy Measurements

Hezy Cohen,[†,‡] Tomer Sapir,[†,‡] Natalia Borovok,[§] Tatiana Molotsky,[§] Rosa Di Felice,[||] Alexander B. Kotlyar,[*,§] and Danny Porath[*,‡]

Physical Chemistry Department and Center for Nanoscience and Nanotechnology, The Hebrew University, Jerusalem 91904, Israel, Department of Biochemistry George S. Wise Faculty of Life Sciences and Nanotechnology Center, Tel Aviv University, Ramat Aviv 69978, Israel, and National Center on nanoStructures and bioSystems at Surfaces (S3) of INFM-CNR, Via Campi 213/A, 41100 Modena, Italy

Received January 3, 2007; Revised Manuscript Received February 22, 2007

ABSTRACT

G4-DNA, a quadruple helical motif of stacked guanine tetrads, is stiffer and more resistant to surface forces than double-stranded DNA (dsDNA), yet it enables self-assembly. Therefore, it is more likely to enable charge transport upon deposition on hard supports. We report clear evidence of polarizability of long G4-DNA molecules measured by electrostatic force microscopy, while coadsorbed dsDNA molecules on mica are electrically silent. This is another sign that G4-DNA is potentially better than dsDNA as a conducting molecular wire.

Double-stranded DNA (dsDNA) was marked as one of the leading candidates for molecular wires in nanoelectronics. Conductivity measurements in DNA provided, however, diverse results, mainly due to the variability in the measured systems (single molecules, bundles, networks, various lengths and compositions) and to the different measurement conditions (on surfaces, free-standing, chemically or physically connected).[1−3] In most of the measurements the contacts played a major influencing role, and indeed some of the measurements were done by contactless methods.[4,5] High electrical currents through short dsDNA oligomers were recently measured using various experimental setups where the dsDNA was not attached to a solid surface along its axis.[6−10] In contrast, however, *long* (*>40 nm*) single dsDNA molecules *attached to hard surfaces* showed no conductivity[2,3,11−13] or polarizability.[4,5] It was suggested that deformations induced by surface forces impaired the conductivity of dsDNA in the latter experiments.[3,14] G4-DNA, due to its higher structural rigidity,[15,16] is expected to be less influenced by this problem. Moreover, it has a high "surface area" in each tetrad (the molecule cross section) for π-stacking and rich guanine content. These properties make it a good candidate for molecular nanowires in nanoelectronics.

An important aspect of experimental setups for measuring direct electrical transport that limits the ability to measure efficiently the intrinsic molecular properties is the presence of molecule−electrode contacts. In fact, it is known that the quality of the contacts between the molecule and the electrodes strongly affects the efficiency of charge injection from the electrode to the molecule.[7,17,18] Therefore, techniques that allow probing the inherent electrical properties of molecules in the absence of contacts are of paramount importance and are playing an increasingly important role to characterize molecular wires. One versatile and powerful such technique is electrostatic force microscopy (EFM),[19,20] as was recently demonstrated on carbon nanotubes and dsDNA.[5]

The G4-DNA molecules that were characterized in our EFM study were produced according to a recently developed synthesis protocol.[16,21] Details of the synthesis method are given in the Supporting Information: we just note here that the presence of K^+ ions during the production of G4-DNA is crucial to the attainment of quadruplexes that show a polarizability signal.[21] The dsDNA (λ-phage DNA) was purchased from a commercial source (Sigma-Aldrich) and used as a reference. The molecules were deposited on a freshly cleaved mica substrate for the measurements. The morphology, density, and location of the molecules on the surface were determined by atomic force microscope (AFM) topography images in noncontact dynamic mode[22] (Nanotec

* Corresponding authors. E-mail: porath@chem.ch.huji.ac.il; s2shak@post.tau.ac.il.

[†] These authors had an equal contribution.

[‡] Physical Chemistry Department and Center for Nanoscience and Nanotechnology, The Hebrew University.

[§] Department of Biochemistry George S. Wise Faculty of Life Sciences and Nanotechnology Center Tel Aviv University.

[||] National Center on nanoStructures and bioSystems at Surfaces (S3) of INFM-CNR.

10.1021/nl070013b CCC: $37.00
Published on Web 03/13/2007

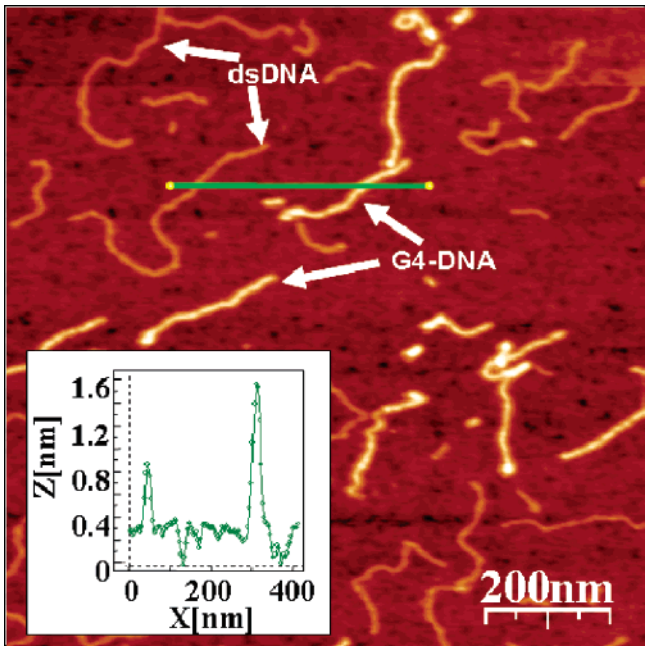

Figure 1. AFM topography image of coadsorbed G4-DNA and dsDNA. A batch of G4-DNA molecules made of ~3200 base poly-(G) strands was imaged here. The inset shows a height profile along the green segment.

Electronica S.L).[23] The enhanced rigidity[16] of G4-DNA with respect to dsDNA is clearly demonstrated in the AFM topography image in Figure 1, where the G4-DNA molecules appear brighter. The line profile in the inset also shows that the apparent height of G4-DNA (~1.2 nm) is about twice larger than that of dsDNA (~0.6 nm),[16] although they have nearly equal nominal diameter (~2.3 nm and ~2.1 nm, respectively).[15] Reduced heights as shown in Figure 1 are common in AFM measurements and are due to the interaction of the molecules with the hard surface.[14] The minor deformation of G4-DNA (40% height reduction) in comparison to dsDNA (70% height reduction) is an index of major resistance to the surface field.

The topography and electrostatic results presented in this paper possess high sensitivity due to the tip characteristics, scanning conditions, and the specific measurement parameters chosen here (see Supporting Information). Two EFM methods were adopted: the "plane mode" and the "3D mode".[24]

The principle of the "plane mode" EFM measurements is sketched in parts a and b of Figure 2. In the "plane mode" operation, the measurement proceeds in two "passes". During the "first pass" a topography image of the sample surface is recorded in noncontact dynamic mode. From this image the tip−sample surface plane parameters are obtained by least-squares fitting. During the "second pass", immediately after the topography imaging, the feedback loop is disconnected, the tip−sample separation is increased to a predefined height above the surface, beyond the van der Waals (VDW) interaction range, and a phase shift image is measured on the same area while the tip is moving on a plane parallel to the surface using the average slope calculated from the "first pass".[25] In order to measure the electrostatic interaction between the tip and the sample, a bias voltage is applied to the tip during the "second pass". When the tip is sampling a region of the surface (e.g., a molecule) with higher polarizability than that of the substrate background, the interaction changes the resonance frequency of the cantilever and consequently shifts the phase of the oscillations, therefore, the detected spatial map of the phase shift is expressive of molecular electrostatic polarizability or of charging. Several sets of scans are normally taken. In consecutive "second passes" the polarity of the bias voltage is positive, negative, or set to zero (a topography image is taken before each "second pass"). If the phase shift is negative (hence reflecting attraction) for both positive and negative voltages, the electrostatic interaction is due to polarizability. Otherwise, if the phase shift is positive for one voltage sign and negative for the opposite voltage sign, then it means that the scanned object (e.g., the molecule) is charged.[26]

The results of our "plane mode" EFM measurements are reported in parts c−f of Figure 2.[27] Figure 2c shows a topography image of a scanned area where molecules of two types, a dsDNA and a G4-DNA, are measured simultaneously. The height difference between the molecules[16] is again clearly seen in the height profile along the green segment, shown in the inset.[28] The "plane mode" method reveals a clear pattern of negative phase shift signal at the position of the G4-DNA when bias voltage was applied to the tip (parts d and f of Figure 2) and no observable signal at 0 V (Figure 2e). The spatial distribution of the signal perfectly coincides with the position of the G4-DNA molecule although it is not uniform along it; the "plane mode" operation is thus able to detect variations of the signal level within a single molecule. This might arise from bending or surface-induced defects or even from inherent nonuniform polarized charge because the object is not purely metallic. The complete absence of signal in the dsDNA is evident. This means that the tip−sample distance was beyond the VDW range, and therefore the phase shift observed over the G4-DNA molecule is a consequence of the electrical interaction solely. The line profiles in the insets show the magnitude of the phase shift at the position of the G4-DNA for both negative and positive tip bias voltages; they also confirm that the phase shift vanishes at the location of the dsDNA irrespective of the bias and at the G4-DNA at zero bias. Although during the "second pass" the tip is closer to the G4-DNA molecule than to the dsDNA, the height difference between them (<1 nm) is much smaller than the tip lift during the "second pass". Consequently, this issue affects the measurement results in a negligible way.

For a continuous tracking of the signal decay as a function of tip−sample distance, we used one of the available combinations of the "three-dimensional (3D) modes".[29] In the "3D mode", the decay of the electrostatic force signal is measured along a pre-fixed line parallel to the sample surface as a function of the tip−sample separation. First, a topography image of the sample is taken to monitor the distribution of the coadsorbed molecules. Then, a line crossing a G4-DNA and a dsDNA in parallel orientation is chosen, the

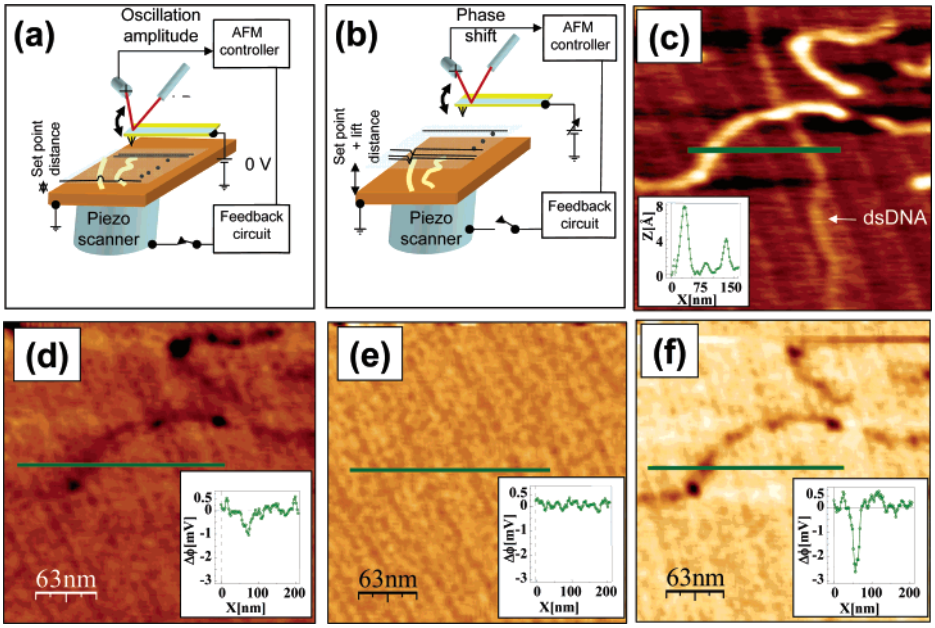

Figure 2. (a and b) Schematic views of the EFM "plane mode" method. (a) A topography image is acquired and its plane parameters are recorded. (b) Then, the tip is lifted and the phase shift is measured with disconnected feedback at lifted height parallel to the previous image plane, with various bias voltages applied to the tip. (c) AFM topography image of the measured coadsorbed G4-DNA (a batch of G4-DNA molecules made of ~3200 base poly(G) strands was used) and dsDNA with a cross section showing the height profile of the molecules. The G4-DNA appears about twice higher than the dsDNA. (d−f) Phase shift images of the same area in plane mode at −3 V (d), 0 V (e), and +3 V (f), showing clearly that the phase signal shifts only above the location of the G4-DNA and only when applying bias voltage. The tip was lifted by 14 nm above the set point value, which was ~20 nm above the surface, as extracted from the force−distance (F−Z) calibration. The negative phase shift, presented in millivolts, indicates a decrease in the frequency of the tip oscillations. Line profiles show the magnitude of the signals at the different voltages (insets).

feedback is disconnected, and the tip is scanned along the line. After each pass the tip−sample separation is increased and the phase shift signal is recorded. The result is a data set where the phase shift, $\Delta\phi(x,z)$, is measured as a function of tip position along the selected line (x) and the tip−sample distance (z).

The principle and the results of the 3D mode experiment are presented in Figure 3. The topography image in Figure 3b was taken prior to the 3D mode scan. The green segment indicates the line along which the 3D mode scan is conducted. The cross section along this segment (Figure 3c) again clearly shows different heights for the dsDNA and the G4-DNA. Three phase-shift maps obtained in the 3D mode measurements are presented in panels d, e, and f of Figure 3 for 0, −3, and +3 V, respectively. The line profiles from these measurements, across the vertical lines of panels d−f of Figure 3, are shown in parts g−i of Figure 3; these profiles represent the phase shift signals as the tip−sample distance increases. As expected, Figure 3g shows that no polarization is detected in the absence of bias voltage on both dsDNA (green) and G4-DNA (red). Clear polarization (negative phase shift) is observed for the G4-DNA at both negative (Figure 3h) and positive (Figure 3i) bias voltages, confirming the "plane mode" results.[30] The 3D mode images demonstrate that as the tip−sample separation increases beyond the VDW range, the electrostatic interaction remains the only relevant origin of the phase shift, which is decaying as a function of tip−sample separation until the signal drops to the noise level over 30 nm above the set point distance.

For a more quantitative analysis, we compare horizontal line profiles (black lines in panels d−f of Figure 3) of G4-DNA and dsDNA at the same tip−sample separation. For panels h and i of Figure 3 this elevation corresponds to elevation h_{80} (see also Figure 4) where the G4-DNA signal presents a decay of 80% of the maximal phase shift magnitude. When a −3 V (+3 V) bias is applied to the tip, the 80% decay for the G4-DNA molecule is achieved at ~18 (20) nm elevation above the set point; at the same elevation no signal is detected on the dsDNA molecule (Figure 3h (Figure 3i)). The phase shift profiles along the horizontal black cross sections, which go across both the dsDNA and the G4-DNA on the sampled area, are presented in parts j−l of Figure 3 at a fixed tip elevation of 40 nm above the surface, close to h_{80}; in this case the G4-DNA signal is weak, slightly above the noise level, and the dsDNA signal is not detectable. We note that, as in the "plane mode", the vertical distance where the electrostatic response is measured is much greater than the height difference between the two types of molecules. In all the comparisons we used force−distance measurements to calibrate the data to the tip deflection due to voltage application.

To further investigate the polarizability signal elicited from G4-DNA molecules, we present in Figure 4 the analysis as a function of the molecular length, obtained from a 3D mode EFM experiment. The molecular length was estimated from AFM topographic images taken prior to the electrostatic measurements. In Figure 4b we define the h_{80} parameter adopted to monitor the length dependence of the polariz-

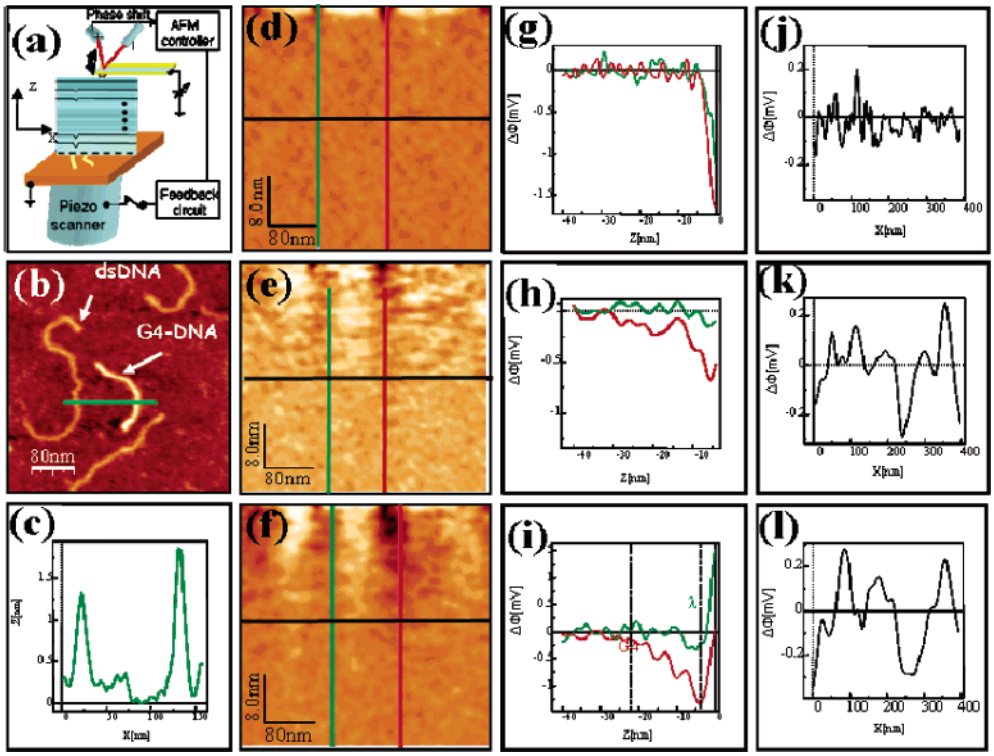

Figure 3. (a) Schematic view of the EFM "3D mode" method along a chosen scanning line (broken line), vertically to the surface. (b) AFM topography image showing dsDNA (left) and G4-DNA (right), and (c) height profile along the green segment that crosses the two imaged molecules. A batch of G4-DNA molecules made of ~3200 base poly(G) strands was used (see the Supporting Information about the synthesis). (d−f) The same segment is also the line at which the 3D mode scans were conducted, at 0 V (d), −3 V (e), and +3 V (f). (g−i) Three sets of line profiles show the phase shift decay as a function of tip−sample separation on G4-DNA (red) and dsDNA (green) at 0 V (g), −3 V (h), and +3 V (i). None of the cross sections shows a signal on the dsDNA, while the G4-DNA shows a clear signal when applying bias voltage (note that the height is calibrated for tip bending using the F−Z measurements). The horizontal cross sections in parts d−f, presented in parts j−l, show the magnitude of the phase shift on both molecules at 40 nm tip−sample separation for comparison. The color code in the curves presented in panels g−l is the same as defined by the vertical and horizontal lines in panels d−f.

ability. The curve represents a phase shift profile taken along the vertical segment of Figure 4a. The different tip−sample distance regimes are highlighted: at very short distances (VDW, black squares) VDW forces are dominant; at intermediate distances a regime where both VDW and electrostatic forces (VDW + ES, red dots) are active is followed by one in which only electrostatic forces survive (ES, green triangles); at very large distances the signal falls into the noise (blue triangles).[31] The range in which EFM measurements are analyzed is the ES regime. The height h_{80} is plotted against the molecule length in Figure 4c: all the points relative to phase shift measurements under voltage (+3 or −3 V) fall around a straight line, indicating that h_{80} monotonically increases with the length of the molecule; on the contrary, no trend is observed if no bias is applied to the tip. Although the precise relation between h_{80} and the corresponding phase shift magnitude is not known, it seems intuitive that the stronger the sample polarizability, the stronger the phase shift at any given height, and consequently the elevation to obtain the 80% reduction is higher. Therefore, if h_{80} increases with the molecule length, one can reasonably deduce that the polarizability is increasing with length.

We now give a rationale of the latter observation by means of a simple electrostatic model. Under the effect of the charged tip, the mobile charges in the molecule are polarized in such a way that charges of opposite sign (relative to the tip) are attracted toward the tip. As a consequence, an attractive molecule−tip force is generated. The absolute value of the phase shift measured in an EFM experiment is proportional to the derivative of this force with respect to the tip−sample distance.[5,29,32] It can be computed and compared to the measured quantity if the induced molecular charge is known. To determine the three-dimensional induced charge on a dielectric object such as a molecule, one cannot rely on the method recently proposed for a metallic carbon nanotube.[32] We thus reduced the problem to a one-dimensional (1D) case (see Figure 4d) and adopted general viable criteria for the induced 1D charge distribution $\lambda(x)$, giving up the precise numerical simulation of the experiment and restraining ourselves to the general understanding of the scaling of the EFM signal with the length of the molecule. The force exerted by our polarizable object on the tip results from the electric field (E_x,E_z) generated by $\lambda(x)$. If the tip is located at $x = 0$ (Figure 4d), which respects the measurement conditions with a good accuracy, then only the z component of the electric field matters, whereas $E_x = 0$. E_z is given by the following relation, with coordinates as defined in Figure 4d (for details see Supporting Information):

$$E_z = \frac{z}{4\pi\epsilon_0}\int_{-a}^{a}\frac{\lambda(s)\,ds}{[(x-s)^2+z^2]^{3/2}}$$

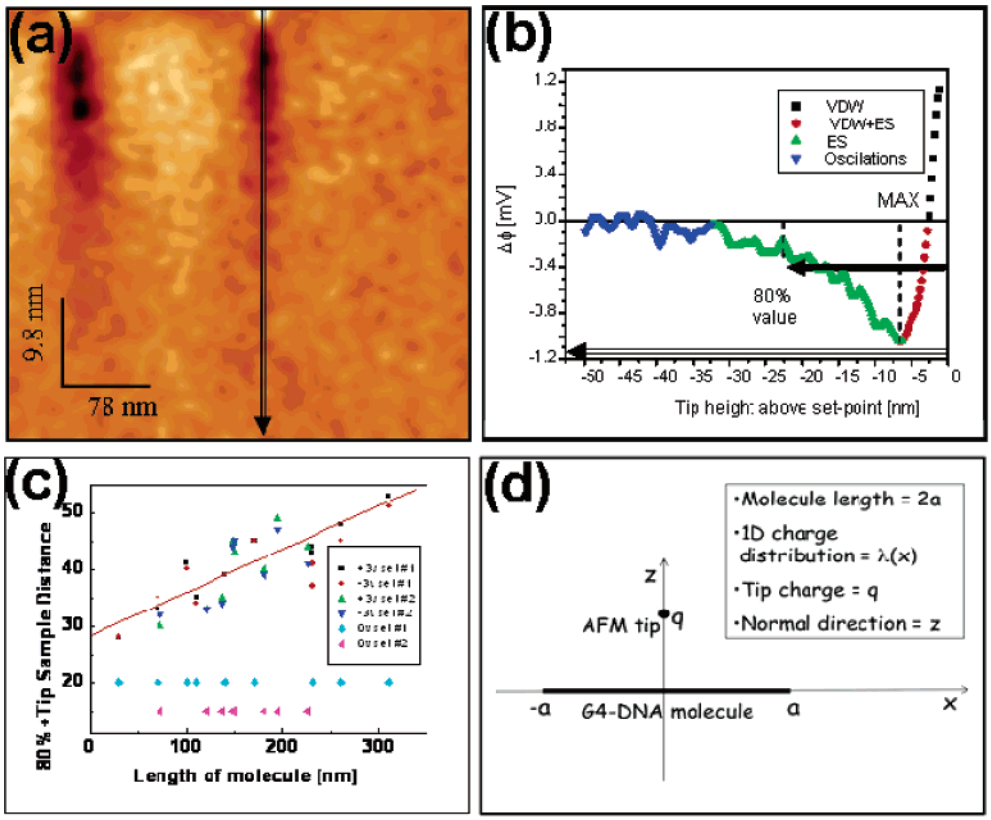

Figure 4. (a) 3D mode phase image of two G4-DNA molecules, employed to define the different interaction regimes. (b) Phase profile taken along the arrow drawn on one of the imaged molecules; the four different regimes of tip−sample separations are defined. The solid arrow defines the h_{80} quantity, namely, the tip height above the set point at which the phase signal (absolute value of the negative phase shift) is reduced to 80% of its maximum absolute value. (c) Plot of h_{80} against the molecules length. (d) Scheme of the electrostatic model adopted to justify the increase of the phase shift with the molecule length. x is the direction along a scanned molecule. The "3D mode" scan occurs in the yz plane, differently from the choice of Figure 3 where the scanning plane is xz. A 1D charge distribution is induced on the molecule by the charge on the tip, which is assumed pointlike for simplicity. The 1D charge distribution generates an electric field in the generic point of the plane xz, and therefore an attractive force F_e on the tip located in the middle of the molecule. The derivative of F_e is proportional to the phase shift.

In order to evaluate this expression, one still needs an estimate of $\lambda(s)$; s coincides with the variable x taken between the edges of the molecule, $-a$ and a in Figure 4d. Such an estimate not only is elusive to electrostatics numerical simulation[32] but also is beyond the possibilities of the EFM measurements and of quantum-chemistry calculations for an adsorbed molecule. For our qualitative purpose, we employed an analytical nonuniform charge distribution $\lambda(s)$ with accumulation of charge just below the tip apex, increasing quadratically with s from the edges to the center of the molecule, in a symmetrical way (Supporting Information). With this particular dependence, the functional behavior of the z derivative of the force between the molecule and the tip is dominated by the term $a \ln z^{-2}(z^2 + a^2)$. Namely, the absolute value of the phase shift (Supporting Information) is growing with the molecule length. Analyzing the integral that defines the electric field (equation above), one realizes that a growing behavior of the force derivative versus a is compatible with any $\lambda(s)$ which scales with a leading power of s greater than 2. The formulas become much more complicated when considering a charge distribution of a realistic shape on the tip, but the qualitative arguments that account for the length scaling still hold. The nonuniformity of the induced polarization charge along the molecule is intuitively justified by the possibility of longitudinal charge motion. Whereas the accumulation of charge just below the tip is an assumption in the model, the viability of this hypothesis rests on robust facts. First, based on the observed EFM negative phase shift, which is indicative of tip−molecule attraction, one can infer that, as expected, the induced charge on the molecule is indeed opposite to the inducing charge on the tip. Second, in a situation in which charges can flow through the axis of the molecule, the molecular 1D charge distribution is optimized to minimize the electrostatic energy, hence with maximum induced charge at a minimum distance from the tip apex oppositely charged, namely, at $x = 0$.

We remark that similar EFM results were observed for eight consecutive batches of G4-DNA prepared with the protocol described in the Supporting Information. Interestingly, G4-DNA that was prepared without the 10 mM KCl during the folding step (step 3) of the synthesis protocol failed to show an EFM signal (data not shown), suggesting that K^+ ions play a key role in making G4-DNA electrically active.

Finally, to further validate our results, we applied the same techniques to single-walled carbon nanotubes (CNTs), which are strongly polarizable objects and therefore constitute good

benchmarks.[4,5] The results on the CNT polarizability (presented in the Supporting Information) are consistent with the results of scanning capacitance microscopy (SCM) experiments on CNTs reported by other groups,[4,20] signifying the reliability and accuracy of the methods adopted here for the DNA measurements.

In conclusion, we have demonstrated the polarizability of single G4-DNA molecules, by precise EFM experiments. In contrast, we found that dsDNA gives no observable polarizability signal, similar to previous results.[3−5] The data are consistent with a model of a nonuniform longitudinal charge distribution along the molecule, which takes into account the possibility of longitudinal charge motion. Although the polarizability is only a qualitative index of charge mobility, a viable hypothesis based on our results and on structural traits is that transport experiments may reveal a higher conductivity for G4-DNA than for dsDNA, thus identifying a new potential molecular wire.

Acknowledgment. We thank Cristina Gómez-Navarro and Julio Gómez Herrero for helpful discussions. We thank Ignacio Horcas and Igor Brodsky for technical assistance. We acknowledge financial support from the European Union through IST Future and Emerging Technologies projects: DNA NANOWIRES and DNA NANODEVICES.

Supporting Information Available: Descriptions of the synthesis, sample preparation, measurement parameters, and calculations and figures showing EFM measurements of a CNT ring and force−distance, amplitude−distance, and $\Delta\phi$−distance curves for the EFM. This material is available free of charge via the Internet at http://pubs.acs.org.

References

(1) Dekker, C.; Ratner, M. A. *Phys. World* **2001**, *14* (8), 29−33.
(2) Endres, R. G.; Cox, D. L.; Singh, R. R. P. *Rev. Mod. Phys.* **2004**, *76* (1), 195−214.
(3) Porath, D.; Cuniberti, G.; Di Felice, R. Charge transport in DNA-based devices. In *Long-Range Charge Transfer in DNA II*; Topics in Current Chemistry 237; Springer: Berlin, 2004; pp 183−227.
(4) Bockrath, M.; Markovic, N.; Shepard, A.; Tinkham, M.; Gurevich, L.; Kouwenhoven, L. P.; Wu, M. S. W.; Sohn, L. L. *Nano Lett.* **2002**, *2* (3), 187−190.
(5) Gomez-Navarro, C.; Moreno-Herrero, F.; de Pablo, P. J.; Colchero, J.; Gomez-Herrero, J.; Baro, A. M. *Proc. Natl. Acad. Sci. U.S.A.* **2002**, *99* (13), 8484−8487.
(6) Cohen, H.; Nogues, C.; Naaman, R.; Porath, D. *Proc. Natl. Acad. Sci. U.S.A.* **2005**, *102* (33), 11589−11593.
(7) Cohen, H.; Nogues, C.; Ullien, D.; Daube, S.; Naaman, R.; Porath, D. *Faraday Discuss.* **2006**, *131*, 367−376.
(8) Nogues, C.; Cohen, S. R.; Daube, S. S.; Naaman, R. *Phys. Chem. Chem. Phys.* **2004**, *6* (18), 4459−4466.
(9) van Zalinge, H.; Schiffrin, D. J.; Bates, A. D.; Haiss, W.; Ulstrup, J.; Nichols, R. J. *ChemPhysChem* **2006**, *7* (1), 94−98.
(10) Xu, B. Q.; Zhang, P. M.; Li, X. L.; Tao, N. J. *Nano Lett.* **2004**, *4* (6), 1105−1108.
(11) Braun, E.; Eichen, Y.; Sivan, U.; Ben-Yoseph, G. *Nature* **1998**, *391* (6669), 775−778.
(12) de Pablo, P. J.; Moreno-Herrero, F.; Colchero, J.; Gomez-Herrero, J.; Herrero, P.; Baro, A. M.; Ordejon, P.; Soler, J. M.; Artacho, E. *Phys. Rev. Lett.* **2000**, *85* (23), 4992−4995.
(13) Storm, A. J.; van Noort, J.; de Vries, S.; Dekker, C. *Appl. Phys. Lett.* **2001**, *79* (23), 3881−3883.
(14) Kasumov, A. Y.; Klinov, D. V.; Roche, P. E.; Gueron, S.; Bouchiat, H. *Appl. Phys. Lett.* **2004**, *84* (6), 1007−1009.
(15) Davis, J. T. *Angew. Chem., Int. Ed.* **2004**, *43* (6), 668−698.
(16) Kotlyar, A. B.; Borovok, N.; Molotsky, T.; Cohen, H.; Shapir, E.; Porath, D. *Adv. Mater.* **2005**, *17* (15), 1901−1905.
(17) Salomon, A.; Cahen, D.; Lindsay, S.; Tomfohr, J.; Engelkes, V. B.; Frisbie, C. D. *Adv. Mater.* **2003**, *15* (22), 1881−1890.
(18) Dadosh, T.; Gordin, Y.; Krahne, R.; Khivrich, I.; Mahalu, D.; Frydman, V.; Sperling, J.; Yacoby, A.; Bar-Joseph, I. *Nature* **2005**, *436* (7051), 677−680.
(19) Schonenberger, C. *Phys. Rev. B* **1992**, *45* (7), 3861−3864.
(20) Staii, C.; Johnson, A. T.; Pinto, N. J. *Nano Lett.* **2004**, *4* (5), 859−862.
(21) Borovok, N.; Molotsky, T.; Ghabboun, J.; Porath, D.; Kotlyar, A. Submitted for publication.
(22) de Pablo, P. J.; Colchero, J.; Luna, M.; Gomez-Herrero, J.; Baro, A. M. *Phys. Rev. B* **2000**, *61* (20), 14179−14183.
(23) Horcas, I.; Fernandez, R.; Gomez-Rodriguez, J. M.; Colchero, J.; Gomez-Herrero, J.; Baro, A. M. *Rev. Sci. Instrum.* **2007**, *78*, 013705.
(24) An issue of major importance for both plane mode and 3D mode is the tip−sample separation that is extracted from force−distance (F−Z) and amplitude−distance (A−Z) curves. Analysis of both F−Z and A−Z curves is provided in the Supporting Information.
(25) Since the feedback is disconnected for a longer time than in lift mode, the plane mode operation should be practiced on a flat surface and small area, as in our measurements.
(26) Some of the molecules were measured for comparison and verification of the results also using the retrace method (as in refs 4 and 5), where the tip is lifted after every line for phase detection and by using retrace with no lift but only with amplitude reduction. The correctness of the employed parameters was checked by F−Z and A−Z also here as in the rest of the work.
(27) The image processing in parts c, e, and g of Figure 2 included truncation of the signal and application of offset, to show them all at the same signal range. It was done to achieve a more reliable comparison of the relative magnitudes when looking at the images.
(28) The actual heights may differ due to different tip and scanning conditions.
(29) Gomez-Navarro, C.; Gil, A.; Alvarez, M.; De Pablo, P. J.; Moreno-Herrero, F.; Horcas, I.; Fernandez-Sanchez, R.; Colchero, J.; Gomez-Herrero, J.; Baro, A. M. *Nanotechnology* **2002**, *13* (3), 314−317.
(30) In particular, it confirms that the height at which the plane mode was measured was indeed beyond the VDW range.
(31) Obviously the separation between the various regimes is not sharp as marked by the colors which are just to guide the reader.
(32) Sacha, G. M.; Gomez-Navarro, C.; Saenz, J. J.; Gomez-Herrero, J. *Appl. Phys. Lett.* **2006**, 89, 173122−1/3.

NL070013B